Synthesis, characterization and in vitro cytotoxicity of the first palladium(II) oxalato complexes involving adenine-based ligands

ARTICLE *in* JOURNAL OF INORGANIC BIOCHEMISTRY · JUNE 2009

Impact Factor: 3.44 · DOI: 10.1016/j.jinorgbio.2009.04.008 · Source: PubMed

3 AUTHORS, INCLUDING:

Pavel Starha
Palacký University of Olomouc
42 PUBLICATIONS **260** CITATIONS
SEE PROFILE

Igor Popa
Palacký University of Olomouc
59 PUBLICATIONS **587** CITATIONS
SEE PROFILE

Journal of Inorganic Biochemistry 103 (2009) 978–988

Contents lists available at ScienceDirect

Journal of Inorganic Biochemistry

journal homepage: www.elsevier.com/locate/jinorgbio

Synthesis, characterization and *in vitro* cytotoxicity of the first palladium(II) oxalato complexes involving adenine-based ligands

Pavel Štarha, Zdeněk Trávníček *, Igor Popa

Department of Inorganic Chemistry, Faculty of Science, Palacký University, Křížkovského 10, CZ-771 47 Olomouc, Czech Republic

ARTICLE INFO

Article history:
Received 7 November 2008
Received in revised form 27 February 2009
Accepted 20 April 2009
Available online 4 May 2009

Keywords:
Palladium(II) complexes
Oxalate
Adenine derivatives
In vitro cytotoxicity
X-ray structure

ABSTRACT

The first $[Pd(L^n)_2(ox)]$ xH_2O oxalato(ox) complexes involving 2-chloro-N6-(benzyl)-9-isopropyladenine (L^1; complex **1**), 2-chloro-N6-(4-methoxybenzyl)-9-isopropyladenine (L^2; **2**), 2-chloro-N6-(2,3-dimethoxybenzyl)-9-isopropyladenine (L^3; **3**), 2-chloro-N6-(2,4-dimethoxybenzyl)-9-isopropyladenine (L^4; **4**), and 2-chloro-N6-(4-methylbenzyl)-9-isopropyladenine (L^5; **5**) have been synthesized by the reactions of potassium bis(oxalato)palladate(II) dihydrate, $[K_2Pd(ox)_2]\cdot 2H_2O$, with the mentioned organic compounds (H_2ox = oxalic acid; $x = 0$ for **1**–**3** and **5** or 2 for **4**). Elemental analyses (C, H, N), FTIR, Raman and NMR (^1H, ^{13}C, ^{15}N) spectroscopies, conductivity measurements and thermal studies (thermogravimetric and differential thermal analyses, TG/DTA) have been used to characterize the prepared complexes. The molecular structures of $[Pd(L^2)_2(ox)]$ (**2**) and $[Pd(L^5)_2(ox)]\cdot L^5\cdot Me_2CO$ (**5**·L^5·Me_2CO) have been determined by a single crystal X-ray analysis. The geometry of these complexes is slightly distorted square-planar with two appropriate L^n ($n = 2$ or 5) molecules mutually arranged in the head-to-head (**2**) or head-to-tail (**5**) orientation. The L^n ligands are coordinated to the central Pd(II) ion *via* the N7 atoms. The same conclusions regarding the binding properties of L^1–L^5 ligands can be made based on multinuclear NMR spectra. *In vitro* cytotoxicity of the complexes **1**–**5** has been evaluated against human chronic myelogenous leukaemia (K562) and human breast adenocarcinoma (MCF7) cancer cell lines. Significant cytotoxicity has been determined for the complexes **3** (IC_{50} = 6.2 μM) and **5** (IC_{50} = 6.8 μM) on the MCF7 cell line, which is even better than that found for the well-known and widely-used platinum-bearing antineoplastic drugs, i.e. oxaliplatin and cisplatin.

1. Introduction

The preparations of metallocomplexes with potential antitumor activity has been one of the main targets of transition metal chemistry since Rosenberg's discovery of cisplatin {*cis*-diamminedichloridoplatinum(II), *cis*-$[Pt(NH_3)_2Cl_2]$} cytotoxic activity in the 1960s [1]. In 1978, cisplatin was approved as the first platinum-based drug for the oncology treatment, although several negative side-effects (nephrotoxicity, neurotoxicity, nausea, etc.) had been induced on treated patients [2]. Nevertheless, cisplatin was followed by carboplatin [3] {*cis*-diammine-1,1-cyclobutanedicarboxylateplatinum(II), $[Pt(NH_3)_2(cbdc)]$, approved in 1985} and oxaliplatin [4] {*1R*,*2R*-diamminocyclohexaneoxalatoplatinum(II), [Pt(dach)(ox)], approved in 1996}, which met requirements of improving antitumor activity and reducing disadvantages of cisplatin. carboplatin and oxaliplatin represent the second, and third platinum-based drug generations, respectively [5].

Nowadays, not only platinum-bearing complexes are extensively studied with the aim to broaden a spectrum of transition metal-based complexes which could be used in the treatment of cancer. Mainly due to the similar structural properties, palladium(II) complexes were tested on various cancer cells among the first of the non-platinum metallocomplexes. The simple analogues of effective antitumor platinum(II) complexes, such as *cis*-$[Pd(NH_3)_2Cl_2]$ and $[Pd(dach)_2Cl_2]$, have been prepared and tested, however, they were found to be inactive on a Sarcoma 180 tumour cell line [6].

Up to now, many mono-, di-, or polynuclear palladium(II) complexes with various N-donor or S-donor ligands have been reported as agents with promising properties for the cancer therapy [7,8]. For instance, the *trans*-$[Pd(dmnp)_2Cl_2]$ complex (dmnp = 2,6-dimethyl-4-nitropyridine) exceeds the antitumor activity of cisplatin in *in vitro* testing on the adenocarcinoma of the rectum (SW707), breast cancer (T47D) and bladder cancer (HCV29T) human cell lines, with the IC_{50} (the drug concentrations lethal for 50% of the tumour cells) values of 1.1, 1.0, and 1.1 μM, respectively, compared to 6.1, 20.0 and 8.1 μM (converted from μg mL^{-1} to μM) as determined for cisplatin on the

* Corresponding author. Tel.: +420 585 634 944; fax: +420 585 634 954.
E-mail address: zdenek.travnicek@upol.cz (Z. Trávníček).

0162-0134/$ - see front matter © 2009 Elsevier Inc. All rights reserved.
doi:10.1016/j.jinorgbio.2009.04.008

same cell lines [9]. The *trans*-[Pd(bbiy)$_2$Cl$_2$] complex (bbiy = 1-benzyl-3-*tert*-butylimidazol-2-ylidene) has been recently reported as a compound, whose cytotoxicity exceeds cisplatin in *in vitro* tests on the HeLa (cervical cancer), MCF7 and HCT 116 (colon adenocarcinoma) human cell lines [10]. Its IC_{50} values (for cisplatin in parentheses) were determined to be 4.0 (8.0), 0.8 (16.0) and 1.0 (15.0) μM on the named cell lines. In our laboratory, other cytotoxic active *trans*-palladium(II) complexes with a PdN_2Cl_2 donor set {*trans*-[Pd(L)$_2$Cl$_2$]·H$_2$O; L = 2-[(*R*)-(1-ethyl-2-hydroxyethylamino)]-N6-(3-hydroxybenzyl)-9-isopropyladenine or 2-[(1-isopropyl-2-hydroxyethylamino)]-N6-(3-hydroxybenzyl)-9-isopropyladenine} were prepared [11]. These complexes were found to be even more active than both cisplatin (IC_{50} = 11 μM) and oxaliplatin (IC_{50} = 18 μM) on the MCF7 human cancer cell line, since their IC_{50} values equalled 3 μM in both cases.

It has been proved for platinum(II) cytotoxic complexes that the oxalato group as well as the chlorido ligands may be considered to be very suitable leaving groups in such complexes [12,13]. Considering this finding, it is quite surprising that only a few monomeric palladium(II) oxalato complexes with a PdN_2O_2 donor set, e.g. [Pd(NH$_3$)$_2$(ox)] [14], [Pd(mi)$_2$(ox)]·2H$_2$O (mi = N-methylimidazole), [Pd(ei)$_2$(ox)] (ei = N-ethylimidazole), [Pd(pi)$_2$(ox)] (pi = N-propylimidazole) [15], [Pd(mi)$_2$(ox)]·H$_2$O [16], [Pd(hoen)$_2$(ox)]·½H$_2$O (hoen = *N,N′*-bis(hydroxyethyl)ethylenediamine) and [Pd(clen)$_2$(ox)] (clen = *N,N′*-bis(chloroethyl)ethylenediamine) [17], [Pd(py)$_2$(ox)] (py = pyridoxine, pyridoxial, or pyridoxamine) [18], [Pd(dach)$_2$(ox)] [19], [Pd(phen)(ox)]·H$_2$O (phen = 1,10-phenanthroline) [20], or [Pd(pda)(ox)]·H$_2$O (pda = propane-1,3-diamine) [21] have been reported up to now. To date, twenty X-ray structures with a Pd(ox) motive have been deposited at the Crystallographic Structural Database (CSD ver. 5.29, August 2008 update) [22]. Among them, there are only five monomeric palladium(II) oxalato complexes with a PdN_2O_2 chromophore, i.e. [Pd(NH$_3$)$_2$(ox)] [14], [Pd(mi)$_2$(ox)]·H$_2$O [16], [Pd(py)$_2$(ox)] (py = pyridoxine) [18], [Pd(phen)(ox)]·H$_2$O [20] and [Pd(pda)(ox)]·H$_2$O [21]. With respect to these statements we report the structures of **2** and **5**·L^5·Me$_2$CO as the first examples of palladium(II) complexes involving combination of an oxalate dianion and adenine-based derivative. The above mentioned complexes [Pd(hoen)$_2$(ox)]·½H$_2$O and [Pd(clen)$_2$(ox)] were tested for their antitumour activity, but they were found inactive on P388 (mice leukaemia) cells with the IC_{50} values equal to 200 μM. Finally, it is necessary to mention some of the mononuclear palladium(II) complexes with purine-based N-donor ligands, such as *trans*-[Pd(nuo)$_2$X$_2$]·*x*H$_2$O (nuo = adenosine, guanosine, inosine, or xanthosine, X = Cl$^-$ or Br$^-$) [23], *cis*-[Pd(pen)$_2$Cl$_2$] (pen = 2-amino-9-[4-hydroxy-3-(hydroxymethyl)-butyl]-6,9-dihydro-3*H*-purin-6-one, penciclovir) [24], *trans*-[Pd(ade)$_2$-(bup)$_2$] (AdeH = adenine, bup = tri-*n*-butylphosphine) [25], or [Pd(guo)$_2$(en)] 9H$_2$O (en = ethylene-1,2-diamine) [26].

This paper reports the first palladium(II) oxalato complexes bearing the adenine-based compounds (L^1–L^5) of the general formula [Pd(L^n)$_2$(ox)] ·*x*H$_2$O (**1**–**5**) (*x* = 0 or 2). The compounds L^1–L^5 stand for the derivatives of the aromatic cytokinin 6-(benzylamino)purine [N6-(benzyl)adenine, Bap] [27] and represent the cytotoxic inactive precursors for the preparation of cyclin dependent kinase (CDK) inhibitors, such as e.g. 2-[(*R*)-(1-ethyl-2-hydroxyethylamino)]-N6-(benzyl)-9-isopropyladenine, *R*-Roscovitine (Seliciclib, CYC202), that is presently tested in 2b-phase of clinical trials on patients with non-small cell lung cancer (NSCLC) [28,29]. The prepared complexes **1**–**5** have been fully characterized by various physical techniques. The single crystal X-ray analysis of [Pd(L^2)$_2$(ox)] (**2**) and [Pd(L^5)$_2$(ox)]·L^5·Me$_2$CO (**5**·L^5·Me$_2$CO) revealed a slightly distorted square-planar geometry in the vicinity of the central atom. Moreover, *in vitro* cytotoxicity of the prepared complexes against two human cancer cell lines (K562 and MCF7) has been evaluated and the results are discussed within the text.

2. Experimental

2.1. Materials

Chemicals and solvents were purchased from Sigma–Aldrich Co., Acros Organics Co., Lachema Co. or Fluka Co. They were used as received, except for dimethyl sulfoxide (DMSO), which was dried using $MgSO_4$.

2.2. Physical measurements

Elemental analyses (C, H, N) were performed on a Flash EA-1112 Elemental Analyser (Thermo Finnigan). Conductivity measurements were carried out on a Cond 340i/SET (WTW) in *N,N′*-dimethylformamide (DMF; 10^{-3} M) and acetone (10^{-3} M) solutions at 25 °C. FTIR spectra were recorded on a Nexus 670 FT-IR (ThermoNicolet) using KBr (400–4000 cm^{-1}) and Nujol (150–600 cm^{-1}) techniques. Raman spectroscopy measurements were performed on a NXR FT-Raman Module (ThermoNicolet) in the range of 150–3750 cm^{-1}. The intensity of reported FTIR and Raman signals are defined as w = weak, m = medium, s = strong and vs = very strong. ^{1}H, ^{13}C and ^{15}N NMR spectra [^{1}H–^{1}H gs-COSY, ^{1}H–^{13}C gs-HMQC, ^{1}H–^{13}C gs-HMBC and ^{1}H–^{15}N gs-HMBC (obtained at natural abundance) at 300 K, and ^{1}H and ^{1}H–^{15}N gs-HMBC also at 340 K in case of all complexes; gs = gradient selected, COSY = correlation spectroscopy, HMQC = Heteronuclear Multiple Quantum Coherence, HMBC = Heteronuclear Multiple Bond Coherence] of DMF-d_7 solutions of L^1–L^5 and **1**–**5** were measured on a Bruker Avance 300 MHz NMR spectrometer at 300.13 MHz, 75.47 MHz and 30.42 MHz for ^{1}H, ^{13}C, and ^{15}N, respectively. Spectra were calibrated against the signals of tetramethylsilane (an internal standard for ^{1}H and ^{13}C NMR spectra) and against the residual signals of the solvent (an internal reference for ^{15}N adjusted to 104.7 ppm). Simultaneous thermogravimetric (TG) and differential thermal (DTA) analyses were carried out using a thermal analyzer Exstar TG/DTA 6200 (Seiko Instruments Inc.). TG/DTA studies were performed in ceramic pans from laboratory temperature to 650 °C (**2** and **3**) or 1000 °C (**1**, **4** and **5**) with a 2.5 °C min^{-1} temperature gradient in dynamic air atmosphere (150 mL min^{-1}).

2.3. Single crystal X-ray analysis of [Pd(L^2)$_2$(ox)] (**2**) and [Pd(L^5)$_2$(ox)]·L^5·Me$_2$CO (**5**·L^5·Me$_2$CO)

X-ray measurements of selected crystals of **2** and **5**·L^5·Me$_2$CO were collected on an Xcalibur™2 diffractometer (Oxford Diffraction Ltd.) with Mo Kα (Monochromator Enhance, Oxford Diffraction Ltd.) and Sapphire2 CCD detector at 120 K, and 105 K, respectively. Data collection and reduction were performed using CrysAlis software (Version 1.171.24) [30]. The structure was solved by direct methods using SHELXS-97 [31] and refined on F^2 using the full-matrix least-squares procedure (SHELXL-97) [32]. Non-hydrogen atoms were refined anisotropically and hydrogen atoms were located in a difference map and refined by using the riding model with C–H = 0.95 and 0.99 Å, N–H = 0.88 Å and U_{iso}(H) = 1.2U_{eq}(CH, CH$_2$, NH) or 1.5U_{eq}(CH$_3$). The isopropyl group of **2**, involving the C(16), C(17) and C(18) atoms, was refined as disordered over two positions with occupancy factors 63% and 37%, while the C(23) atom of acetone molecule of crystallization of **5**·L^5·Me$_2$CO was refined with the occupancy of 50% for each of two components. The molecular graphics were drawn and additional structural parameters were interpreted using DIAMOND [33].

2.4. In vitro cytotoxicity

In vitro cytotoxicity of the complexes **1**–**5** was determined by a calcein acetoxymethyl (AM) assay on the chronic myelogenous leukaemia (K562) and breast adenocarcinoma (MCF7) human cancer cell lines, which were maintained in plastic tissue culture flasks and grown (37 °C, 5% CO_2 atmosphere, 100% humidity) on Dulbecco's modified Eagle's cell culture medium (DMEM). The suspension of cancer cells (*ca* 1.25×10^5 cells mL^{-1}) was reattributed into 96-well microtitre plates (Nunc) and preincubated for 12 h. The tested palladium(II) complexes, which were pre-dissolved in DMF (DMF was used instead of DMSO in connection with high ability of DMSO to coordinate to Pd(II) ion which could cause the substitution of L^n ligands in the tested complexes) and then diluted with deionised water to the final DMF concentration of 0.6%, were added in the concentration range of 0.2–25 μM. After the incubation lasting 72 h, the cells were incubated with calcein AM for 1 h. The fluorescence of the live cells was measured at 485/538 nm (excitation/emission) with Fluoroscan Ascent (Labsystems). Each experiment was repeated three times and the discussed IC_{50} values represent an arithmetic mean. The maximal deviation did not exceed 17% related to an arithmetic mean.

2.5. Syntheses

2.5.1. Syntheses of starting compounds

2.5.1.1. Potassium Bis(oxalato)palladate(II) Dihydrate, $K_2[Pd(ox)_2]\cdot 2H_2O$. $K_2[Pd(ox)_2]\cdot 2H_2O$ was synthesized using a slightly modified and previously published procedure [34]. Both potassium tetrachloropalladate(II), K_2PdCl_4, and potassium oxalate monohydrate, $K_2(ox)\cdot H_2O$, were dissolved separately in a minimum volume of distilled water (25 °C) in a 1:2 molar ratio. Then, both solutions were mixed together and stirred in the dark at laboratory temperature for 1 h. Orange precipitate, which formed, was filtered off and washed with cold distilled water and ethanol. The product was dissolved in a minimum volume of hot distilled water (50 °C), and then cooled down in the fridge to give the orange-brown needle-like crystals of $K_2[Pd(ox)_2]\cdot 2H_2O$ in very good yields (>90%). The compound was characterized by elemental analyses and FTIR, Raman and ^{13}C NMR spectroscopies. *Note: $K_2[Pd(ox)_2]\cdot 2H_2O$ should be stored in the dark and cool place to avoid its decomposition induced by light and heat.* Anal. Calc. for $PdK_2C_4O_8\cdot 2H_2O$ (M_r = 396.7): C, 12.1; H, 1.0. Found: C, 12.3; H, 1.0%. IR (Nujol; cm^{-1}): 562m, 492w, 413w, 372m, 350vs, 291w, 236m, 215m. IR (KBr; cm^{-1}): 3559m, 3469m, 1702vs, 1679vs, 1660s, 1393s, 1236m, 1051w, 897w, 822m, 559m, 471m, 420m. Raman (cm^{-1}): 3492w, 3416w, 1717s, 1663m, 1420m, 1255m, 900w, 847w, 804w, 567m, 243vs. ^{13}C NMR (D_2O, ppm): δ 166.95 (Cox).

2.5.1.2. 2-Chloro-N6-(benzyl)-9-isopropyladenine (L^1), 2-chloro-N6-(4-methoxybenzyl)-9-isopropyladenine (L^2), 2-chloro-N6-(2,3-dimethoxybenzyl)-9-isopropyladenine (L^3), 2-chloro-N6-(2,4-dimethoxybenzyl)-9-isopropyladenine (L^4) and 2-chloro-N6-(4-methylbenzyl)-9-isopropyladenine (L^5). Modification of a formerly reported procedure [35] has been used for the preparation of organic molecules which are summarized in Scheme 1. Briefly, the first step included alkylation of the N9 position of 2,6-dichloropurine by 2-bromopropane provided in dried DMSO at laboratory temperature. Prepared 2,6-dichloro-9-isopropylpurine (DCIP) reacted in ethyl acetate (80 °C; 5 h) with an equimolar amount of benzylamine or its corresponding derivative. The mixture was stirred overnight at laboratory temperature. The solvent was evaporated under vacuum and the formed solid was filtered off, washed by ethyl acetate, distilled water and diethyl ether and dried in the air at the temperature of 40 °C. The results of elemental analyses, FTIR, Raman and NMR (^1H, ^{13}C, ^{15}N) spectral data and structural formulas of L^1–L^5 compounds are summarized in Appendix A in Supplementary material.

*2.5.2. Preparation of $[Pd(L^1)_2(ox)]$ (**1**), $[Pd(L^2)_2(ox)]$ (**2**), $[Pd(L^3)_2(ox)]$ (**3**), $[Pd(L^4)_2(ox)]\cdot 2H_2O$ (**4**) and $[Pd(L^5)_2(ox)]$ (**5**)*

The corresponding organic compound, L^1–L^5, (2 mmol) was dispersed in 5 mL of acetone and added to a water solution (5 mL) of $K_2[Pd(ox)_2]\cdot 2H_2O$ (1 mmol). The reaction mixture was stirred for ca. 24 h at 40 °C. The obtained solid, representing the palladium(II) complexes **1**–**5**, was filtered off, washed with warm and cold distilled water, and *iso*propanol, and dried in the air at 40 °C. Single crystals of **2** were obtained from the acetone solution of **2** in 4 weeks. In the case of **5**, well developed single crystals of $[Pd(L^5)_2(ox)]\cdot L^5\cdot Me_2CO$ (**5**·L^5·Me_2CO) formed in the mother liquor in a few weeks. The results of FTIR, Raman and NMR spectroscopies are summarized in Appendix A in Supplementary material.

1: Yield: 500 mg (63%). Anal. Calc. for $PdC_{32}H_{32}N_{10}O_4Cl_2$ (M_r = 798.0): C, 48.2; H, 4.0; N, 17.6. Found: C, 48.1; H, 3.9; N, 17.1%.

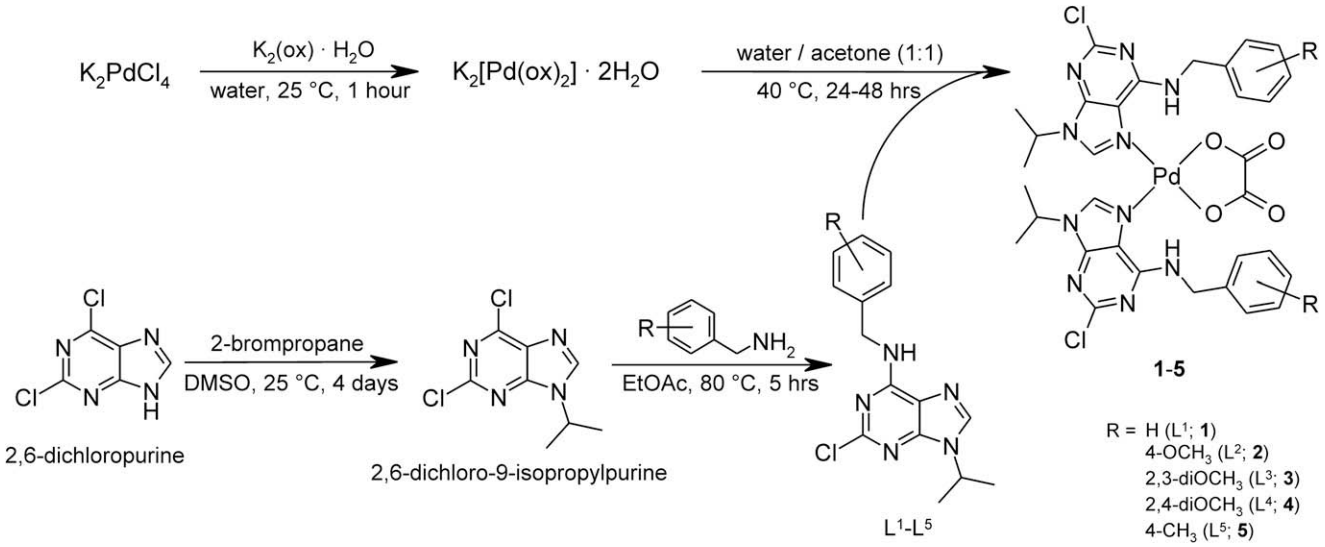

Scheme 1. Synthetic pathways for the preparation of starting compounds, i.e. $K_2[Pd(ox)_2]\cdot 2H_2O$ and L^1–L^5, and palladium(II) complexes (**1**–**5**).

2: Yield: 704 mg (82%). Anal. Calc. for $PdC_{34}H_{36}N_{10}O_6Cl_2$ (M_r = 858.0): C, 47.6; H, 4.2; N, 16.3. Found: C, 47.8; H, 4.2; N, 15.8%.

3: Yield: 740 mg (81%). Anal. Calc. for $PdC_{36}H_{40}N_{10}O_8Cl_2$ (M_r = 918.1): C, 47.1; H, 4.4; N, 15.3. Found: C, 47.5; H, 4.7; N, 15.0%.

4: Yield: 640 mg (70%). Anal. Calc. for $PdC_{36}H_{40}N_{10}O_8Cl_2\ 2H_2O$ (M_r = 954.1): C, 45.3; H, 4.6; N, 14.7. Found: C, 45.5; H, 4.8; N, 15.0%.

5: Yield: 550 mg (67%). Anal. Calc. for $PdC_{34}H_{36}N_{10}O_4Cl_2$ (M_r = 826.0): C, 49.4; H, 4.4; N, 17.0. Found: C, 48.9, H, 4.3; N, 17.3%.

3. Results and discussion

3.1. General properties

Pale yellow palladium(II) complexes $[Pd(L^n)_2(ox)]\cdot xH_2O$ (**1**–**5**) have been synthesized by the reactions of $K_2[Pd(ox)_2]\cdot 2H_2O$ with the corresponding organic derivative (L^1–L^5) in a distilled water/acetone mixture (1:1, v/v) in the 1:2 molar ratio, with quite good yields (63–82%). The complexes **1**–**5** have been found to be very well soluble in DMF, DMSO and acetone, whereas, relatively low solubility has been observed in ethanol, methanol and distilled water at laboratory temperature. The determined values of molar conductivity ranged from 1.1 to 3.8 S cm^2 mol^{-1} (for 10^{-3} M DMF solutions) and from 0.1 to 1.4 S cm^2 mol^{-1} (for 10^{-3} M acetone solutions) (Table 6), and confirmed that the prepared palladium(II) complexes behave as non-electrolytes [36]. The values of molar conductivity were determined as slightly higher after 4 weeks (3.1–8.3 S cm^2 mol^{-1} for DMF solutions and from 2.3–4.0 S cm^2 mol^{-1} for acetone solutions) which can be caused by a partial dissociation of the complexes in the solvents used.

3.2. FTIR and Raman spectroscopy

The presence of both the L^1–L^5 ligands and oxalate dianion in the palladium(II) complexes **1**–**5** has been clearly proved by FTIR and Raman spectroscopy. The bands of very strong intensity detected in the 1614–1619 cm^{-1} region (see Table 2) in the FTIR spectra may be assigned to the ν(C=N) vibration of a purine ring [37]. These bands are shifted by 3–30 cm^{-1} compared with those observed in free L^1–L^5 compounds, showing on coordination of these organic molecules as ligands. The other vibrations characterizing L^2–L^4 ligands (involved in the complexes **2**–**4**) with methoxy-substituted benzyl ring, were observed at 1033–1062 cm^{-1} and 1229–1243 cm^{-1}, which can be assigned to [ν(C–O)$_{met}$, and ν(C–O)$_{ar}$], respectively. The bands observed at 1157–1176 cm^{-1},

Table 1
Crystal data and structure refinements for **2** and **5**·L^5·Me_2CO.

Compound	**2**	**5**·L^5·Me_2CO
Empirical formula	$C_{34}H_{36}Cl_2N_{10}O_6Pd$	$C_{53}H_{60}Cl_3N_{15}O_5Pd$
Formula weight	858.03	1199.91
Temperature (K)	120(2)	105(2)
Wavelength (Å)	0.71073	0.71073
Crystal system, space group	Triclinic, $P\bar{1}$	Triclinic, $P\bar{1}$
Unit cell dimensions		
a (Å)	9.3315(2)	10.8200(3)
b (Å)	13.9014(4)	15.0532(4)
c (Å)	16.0228(5)	17.6293(4)
α (°)	64.671(3)	89.068(2)
β (°)	85.916(2)	75.599(2)
γ (°)	73.535(2)	83.676(2)
V (Å^3)	1798.62(9)	2764.05(12)
Z, D_{calc} (g cm^{-3})	2, 1.584	2, 1.442
Absorption coefficient (mm^{-1})	0.725	0.542
Crystal size (mm)	0.25 × 0.20 × 0.20	0.25 × 0.20 × 0.15
F (0 0 0)	876	1240
θ range for data collection (°)	$2.60 \leqslant \theta \leqslant 25.00$	$2.68 \leqslant \theta \leqslant 25.00$
Index ranges (h, k, l)	$-11 \leqslant h \leqslant 11$	$-12 \leqslant h \leqslant 11$
	$-12 \leqslant k \leqslant 16$	$-17 \leqslant k \leqslant 17$
	$-17 \leqslant l \leqslant 19$	$-20 \leqslant l \leqslant 17$
Reflections collected/unique (R_{int})	15041/6302 (0.0244)	23281/9674 (0.0439)
Max. and min. transmission	0.8686 and 0.8395	0.9231 and 0.8763
Data/restraints/parameters	6302/0/504	9674/0/707
Goodness-of-fit on F^2	1.109	1.020
Final R indices [$I>2\sigma(I)$]	R_1 = 0.0383, wR_2 = 0.0915	R_1 = 0.0474, wR_2 = 0.0961
R indices (all data)	R_1 = 0.0537, wR_2 = 0.1028	R_1 = 0.0783, wR_2 = 0.1030
Largest peak and hole (e Å^{-3})	0.741, −0.587	0.631, −0.815

Table 2
Important FTIR and Raman (in parentheses) data for $K_2[Pd(ox)_2]\cdot 2H_2O$ and complexes **1**–**5** given in cm^{-1}.

Complex	ν(Pd–N)	ν(Pd–O)	ν(C–Cl)	ν(C=C)	ν(C=N)	ν_a(C=O)$_{ox}$	ν(C–H)$_{aliphatic}$
$K_2[Pd(ox)_2]\cdot 2H_2O$	–	562 (567)	–	–	–	1702, 1679 (1717, 1663)	–
1	521 (523)	560 (558)	1164 (1160)	1581, 1486 (1579, 1488)	1617 (1606)	1705, 1676 (1691, 1671)	3060, 2941 (3063, 2943)
2	521 (523)	564 (562)	1157 (1157)	1580, 1483 (1576, 1486)	1614 (1610)	1708, 1676 (1695, 1660)	3061, 2935 (3060, 2950)
3	516 (515)	559 (560)	1169 (1170)	1581, 1480 (1580, 1489)	1619 (1614)	1709, 1677 (1695, 1676)	3068, 2936 (3053, 2935)
4	517 (526)	565 (562)	1157 (1159)	1588, 1485 (1583, 1489)	1618 (1610)	1714, 1672 (1706, 1668)	3062, 2937 (3072, 2933)
5	522 (526)	562 (571)	1163 (1157)	1581, 1483 (1579, 1486)	1617 (1614)	1716, 1674 (1702, 1670)	3057, 2930 (3053, 2941)

Table 3
Selected coordination shifts ($\Delta\delta = \delta_{complex} - \delta_{ligand}$) observed for complexes **1**–**5** in ^{1}H, ^{13}C NMR and ^{1}H-^{15}N gs-HMBC spectra.

Complex	^{1}H NMR		^{13}C NMR						^{15}N NMR				
	N6H	C8H	C2	C4	C5	C6	C8	Cox	N1	N3	N6	N7	N9
1	0.57	0.49	0.12	−0.25	−2.42	−0.93	3.82	−1.07	4.4	0.1	7.1	−92.4	7.1
2	0.46	0.41	−0.02	−0.26	−2.46	−0.84	3.84	−0.98	5.9	2.0	8.3	−91.2	9.0
3	0.63	0.47	−0.13	−0.25	−2.44	−0.97	3.80	−1.28	4.0	−0.3	6.5	−92.4	6.2
4	0.63	0.42	0.11	−0.24	−2.43	−1.00	3.84	−1.52	2.5	−1.3	7.7	−94.0	6.1
5	0.54	0.47	0.07	−0.24	−2.45	−0.91	3.82	−1.18	4.4	[a]	7.3	−92.8	6.9

[a] N3 atom was not observed in the ^{1}H–^{15}N gs-HMBC spectrum of L^5.

Table 4
Selected bond lengths (Å) and angles (°) for complexes **2** and **5**·L^5·Me_2CO.

Compound	$[Pd(L^2)_2(ox)]$ (**2**)	$[Pd(L^5)_2(ox)]\cdot L^5\cdot Me_2CO$ (**5**?$L^5\cdot Me_2CO$)	
Bond lengths		[a]	[b]
Pd(1)–N(7)	2.012(3)	2.023(3)	–
Pd(1)–N(7A)	2.024(3)	2.021(3)	–
Pd(1)–O(1)	1.992(2)	1.971(2)	–
Pd(1)–O(2)	1.987(2)	1.983(2)	–
O(1)–C(21)	1.302(4)	1.332(4)	–
O(2)–C(20)	1.289(4)	1.282(4)	–
O(3)–C(21)	1.215(4)	1.239(4)	–
O(4)–C(20)	1.222(4)	1.230(4)	–
C(20)–C(21)	1.549(5)	1.471(5)	–
N(1)–C(2)	1.321(5)/1.328(5)	1.328(4)/1.315(4)	1.332(4)
N(1)–C(6)	1.355(4)/1.358(4)	1.349(4)/1.345(4)	1.351(4)
C(2)–Cl(1)	1.755(4)/1.756(4)	1.757(4)/1.754(4)	1.751(4)
C(2)–N(3)	1.315(5)/1.303(5)	1.311(4)/1.317(4)	1.309(4)
N(3)–C(4)	1.348(4)/1.350(5)	1.344(4)/1.346(4)	1.353(4)
C(4)–C(5)	1.384(5)/1.382(5)	1.380(5)/1.376(5)	1.381(5)
C(4)–N(9)	1.378(5)/1.352(5)	1.371(4)/1.384(4)	1.375(4)
C(5)–C(6)	1.403(5)/1.417(5)	1.406(5)/1.422(5)	1.408(5)
C(5)–N(7)	1.394(4)/1.390(4)	1.397(4)/1.392(4)	1.397(4)
C(6)–N(6)	1.339(4)/1.319(4)	1.330(4)/1.333(4)	1.335(4)
N(7)–C(8)	1.327(4)/1.319(4)	1.316(4)/1.327(4)	1.313(4)
C(8)–N(9)	1.341(5)/1.347(5)	1.351(4)/1.344(4)	1.363(4)
Bond angles			
O(1)–Pd(1)–N(7A)	93.09(10)	89.86(10)	–
O(1)–Pd(1)–N(7)	174.96(10)	173.26(10)	–
O(1)–Pd(1)–O(2)	84.46(9)	84.20(10)	–
O(2)–Pd(1)–N(7)	91.12(10)	89.38(10)	–
O(2)–Pd(1)–N(7A)	177.10(10)	171.75(10)	–
N(7)–Pd(1)–N(7A)	91.39(11)	96.32(11)	–
Pd(1)–O(1)–C(21)	111.8(2)	110.6(2)	–
Pd(1)–O(2)–C(20)	111.8(2)	111.5(2)	–
O(1)–C(21)–O(3)	125.2(3)	121.1(3)	–
O(2)–C(20)–O(4)	124.9(3)	123.0(3)	–
O(1)–C(21)–C(20)	115.3(3)	116.3(3)	–
O(2)–C(20)–C(21)	115.9(3)	117.4(3)	–
O(3)–C(21)–C(20)	119.5(3)	122.5(3)	–
O(4)–C(20)–C(21)	119.3(3)	119.6(3)	–
Pd(1)–N(7)–C(5)	127.9(2)/129.8(2)	135.8(2)/129.9(2)	–
Pd(1)–N(7)–C(8)	126.9(2)/124.8(2)	119.2(2)/119.6(2)	–
C(2)–N(1)–C(6)	117.4(3)/117.5(3)	116.9(3)/117.4(3)	117.0(3)
N(1)–C(2)–N(3)	131.5(3)/132.1(3)	132.3(3)/132.4(3)	132.1(3)
C(2)–N(3)–C(4)	109.7(3)/109.7(3)	109.4(3)/109.0(3)	109.6(3)
N(3)–C(4)–C(5)	126.4(3)/126.5(4)	126.4(3)/127.2(3)	126.2(3)
N(3)–C(4)–N(9)	127.2(3)/126.4(3)	126.1(3)/126.2(3)	127.5(3)
C(4)–C(5)–C(6)	116.8(3)/117.2(3)	117.5(3)/116.5(3)	117.4(3)
C(4)–C(5)–N(7)	108.8(3)/108.2(3)	108.2(3)/108.9(3)	110.5(3)
C(5)–C(6)–N(1)	117.7(3)/116.9(3)	117.5(3)/117.5(3)	117.7(3)
C(5)–C(6)–N(6)	123.7(3)/123.7(3)	122.3(3)/124.5(3)	122.4(3)
N(1)–C(6)–N(6)	118.6(3)/119.4(3)	120.2(3)/118.0(3)	119.9(3)
C(6)–N(6)–C(9)	122.5(3)/124.8(3)	125.9(3)/122.7(3)	124.0(3)
N(6)–C(9)–C(10)	110.2(3)/111.9(3)	111.8(3)/113.2(3)	114.9(3)
C(5)–N(7)–C(8)	105.2(3)/105.4(3)	105.0(3)/105.3(3)	103.1(3)
N(7)–C(8)–N(9)	112.6(3)/112.2(3)	113.4(3)/112.6(3)	114.8(3)
C(8)–N(9)–C(4)	107.1(3)/107.2(3)	105.8(3)/106.6(6)	105.3(3)

[a] data for both coordinated L^5 molecules (N7 atom involving molecule/N7A atom involving molecule). The values given behind the slash belong to the equivalent interatomic parameter.
[b] Data for L^5 molecule of crystallization assigned to the equivalent interatomic parameter.

3103–3138 cm^{-1} and 3269–3385 cm^{-1} can be assigned to ν(C–Cl), ν(C–H)$_{ar}$, and (N–H), respectively. The maxima of the ν(C–H)$_{aliphatic}$ vibrations were detected in the 2835–3068 cm^{-1} region. The medium to strong ν_{as}(C=O)$_{ox}$ bands of an oxalato group were observed

Table 5
Hydrogen bond parameters (Å, °) for complexes **2** and **5**?$L^5{\cdot}Me_2CO$.

D–H···A	d(D–H)	d(H···A)	d(D···A)	< (DHA)
$[Pd(L^2)_2(ox)]$ (**2**)				
N(6)–H(6)···O(4)^{i}	0.88	2.12	2.805(3)	133.7
$[Pd(L^5)_2(ox)]{\cdot}L^5{\cdot}Me_2CO$ (**5**·$L^5{\cdot}Me_2CO$)				
N(6)–H(6)···O(4)^{i}	0.88	2.07	2.786(4)	138.4
N(6A)–H(6A)···O(4)^{i}	0.88	1.97	2.788(4)	154.4
N(6B)–H(6B)···N(7B)^{ii}	0.88	2.30	3.073(4)	146.2

Symmetry codes: (i) $1-x, 1-y, 1-z$; (ii) $1-x, 1-y, -z$.

in both 1672–1676 cm^{-1} and 1705–1716 cm^{-1} regions, supporting a bidentate coordination of this dianion [38]. The bands connected with the $\nu_{sym}(C{-}O)_{ox}$ vibration were found between 1373 and 1389 cm^{-1}. The maxima observed in the far-FTIR spectra of the complexes **1**–**5** at 559–565 cm^{-1} can be assigned to the ν(Pd–O) vibration. These values correlated very well with those observed for $K_2[Pd(ox)_2]{\cdot}2H_2O$ at 562 cm^{-1} (this work) and 556 cm^{-1} (as reported in the literature [39]). The bands observed at 516–522 cm^{-1} may be assignable to ν(Pd–N) (see Table 2) [40].

Very similar conclusions regarding the presence and coordination mode of the ligands within the complexes **1**–**5** may be drawn from the Raman spectra (Table 2). The most intensive bands, which may be assigned to the stretching vibration of the purine skeleton, appeared in the 1340–1351 cm^{-1} region [41]. They were shifted by 1–17 cm^{-1} as compared with the free L^1–L^5 molecules. The vibrations of medium to strong intensity assignable to $\nu(C{-}H)_{aliphatic}$ $\nu_{sym}(C{-}O)_{ox}$ and ν(Pd–O) were observed in the range of 2933–3072 cm^{-1}, 1404–1413 cm^{-1}, and 558–571 cm^{-1}, respectively. The split maxima at 1660–1706 cm^{-1} and sharp peaks at 1606–1614 cm^{-1} belong to $\nu_{as}(C{=}O)_{ox}$, and ν(C=N), respectively. It is quite surprising, that maxima of the ν(C=N) vibration were not shifted by more than two cm^{-1} in the case of complexes **1**–**5** as compared to free ligands L^1–L^5. The weak ν(Pd–N) vibrations, which were found in the Raman spectra of **1**–**5** around 520 cm^{-1}, correlated well with those detected in the FTIR spectra.

3.3. ^1H, ^{13}C, ^{15}N NMR spectroscopy

^1H, ^{13}C, ^1H–^1H gs-COSY, ^1H–^{13}C gs-HMQC, ^1H–^{13}C gs-HMBC and ^1H–^{15}N gs-HMBC NMR experiments were performed for both free L^1–L^5 and complexes **1**–**5**. The comparison of chemical shifts (δ) observed in the NMR spectra of free compounds L^1–L^5 and palladium(II) complexes, which are interpreted and discussed as coordination shifts $\Delta\delta = \delta_{complex} - \delta_{ligand}$, provided relevant information not only about the composition of the prepared complexes **1**–**5** but also about the coordination mode of the L^1–L^5 ligands to the Pd(II) centre.

The most relevant conclusions may be drawn from ^1H–^{15}N gs-HMBC spectra, which clearly proved the coordination of the L^1–L^5 molecules to the Pd(II) ion through the N7 atom of the purine moiety. This statement is based on coordination shift values ($\Delta\delta$), ranging from −94.0 ppm to −91.2 ppm for the N7 atoms, compared to $|\Delta\delta| < 9.0$ of the others nitrogen atoms (Table 3). The same conclusion may be deduced from the results of ^{13}C NMR and ^1H NMR experiments. The most significant coordination shifts, $|\Delta\delta|$, were observed for C8 (shifted by 3.80–3.84 ppm downfield as compared to free L^1–L^5 compounds) and C5 (shifted by 2.42–2.46 ppm upfield) in ^{13}C NMR spectra and for N6H ($\Delta\delta$ ranged from 0.46–0.63 ppm) and C8H ($\Delta\delta$ = 0.41–0.49 ppm) in ^1H NMR spectra. Larger $\Delta\delta$ values of N6H compared to those of C8H may be caused by the different orientation of the benzyl group of L^n ligands within the complexes compared to free organic molecules. Moreover, the presence of non-bonding contacts (e.g. hydrogen bonds), in which the N6H group should be involved in the DMF-d_7 solutions, could affect the chemical shift values as well. It should be noted that such interactions were observed in the solid state in the X-ray structures of the complexes **2** and **5** (see Section 3.4).

The signal of the oxalate dianion carbons (Cox), that was found in the ^{13}C NMR spectra (D_2O solutions) of $K_2[Pd(ox)_2]{\cdot}2H_2O$ at 166.95 ppm, was also found between 165.43–165.97 ppm in the case of ^{13}C NMR spectra of palladium(II) complexes **1**–**5**. Moreover, these signals were not observed by measuring of ^1H–^{13}C gs-HMQC and ^1H–^{13}C gs-HMBC experiments. The mentioned experiments clearly supported the statement that these signals belong to bidentate coordinated oxalato dianion present in the complexes **1**–**5**.

3.4. X-ray structures of $[Pd(L^2)_2(ox)]$ (**2**) and $[Pd(L^5)_2(ox)]{\cdot}L^5{\cdot}Me_2CO$ (**5**·$L^5{\cdot}Me_2CO$)

The molecular structures of **2** and **5**·$L^5{\cdot}Me_2CO$ were determined by a single crystal X-ray analysis and are depicted in Figs. 1 and 3, respectively. The crystal data and structure refinements are given in Table 1, the selected bond lengths and angles are listed in Table 4, while the hydrogen bond parameters are summarized in Table 5.

The Pd(II) centre of **2** is four-coordinated by two N(7) atoms of two L_2 molecules, and the O(1) and O(2) atoms of the bidentate oxalato group (PdN_2O_2 chromophore). The geometry is slightly distorted square-planar (Fig. 1, Table 4). Both L^2 molecules were found to be mutually arranged in head-to-head orientation.

The Pd(1) atom is situated 0.0109(3) Å out of the least-square plane formed by two N-atoms, originating from two L^2 ligands, and by two O-atoms, originating from the bidentate coordinated oxalate dianion. Two purine rings containing N(7) and N(7A) atoms form a dihedral angle being 86.27(6)°. The dihedral angles formed by the corresponding purine moiety and benzene ring of L^2 ligands were found to be 82.26(8)° for $L^2_{N(7)}$ [$L^2_{N(7)}$ = L^2 molecule involving N(7) atom] and 74.07(9)° for $L^2_{N(7A)}$ [$L^2_{N(7A)}$ = L^2 molecule involving

Table 6
Molar conductivity and selected TG/DTA data of complexes **1**–**5**.

Complex	Conductivity data[a]		TG/DTA thermal studies					
			$[Pd(L_n)_2(ox)]{\cdot}xH_2O \rightarrow PdO$			PdO → Pd		
	DMF	Me_2CO	T (°C)	Δm (%)[b]	DTA (°C)[c]	T (°C)	Δm (%)[b]	DTA (°C)
$[Pd(L^1)_2(ox)]$ (**1**)	3.8 (8.3)	1.1 (4.0)	168–444	84.7/84.2	205 exo, 422 exo	809–840	2.0/1.8	816 endo
$[Pd(L^2)_2(ox)]$ (**2**)	1.8 (5.4)	0.1 (2.6)	177–437	85.7/86.8	197 exo, 413 exo	[d]	[d]	[d]
$[Pd(L^3)_2(ox)]$ (**3**)	1.8 (8.1)	0.4 (2.3)	166–434	86.7/87.4	181 exo, 393 exo	[d]	[d]	[d]
$[Pd(L^4)_2(ox)]{\cdot}2H_2O$ (**4**)	1.1 (5.6)	0.1 (2.5)	66–450	87.2/86.2	100 endo, 134 endo, 178 exo, 423 exo	808–834	1.6/1.6	820 endo
$[Pd(L^5)_2(ox)]$ (**5**)	1.6 (3.1)	1.5 (2.5)	174–444	85.2/84.3	199 exo, 429 exo	819–839	1.9/1.8	830 endo

[a] 10^{-3} M solutions; values determined after 28 days in parentheses.
[b] Calc./Found.
[c] Stands for maximum of exothermic effect or minimum of endothermic effect.
[d] Measured up to 650 °C only.

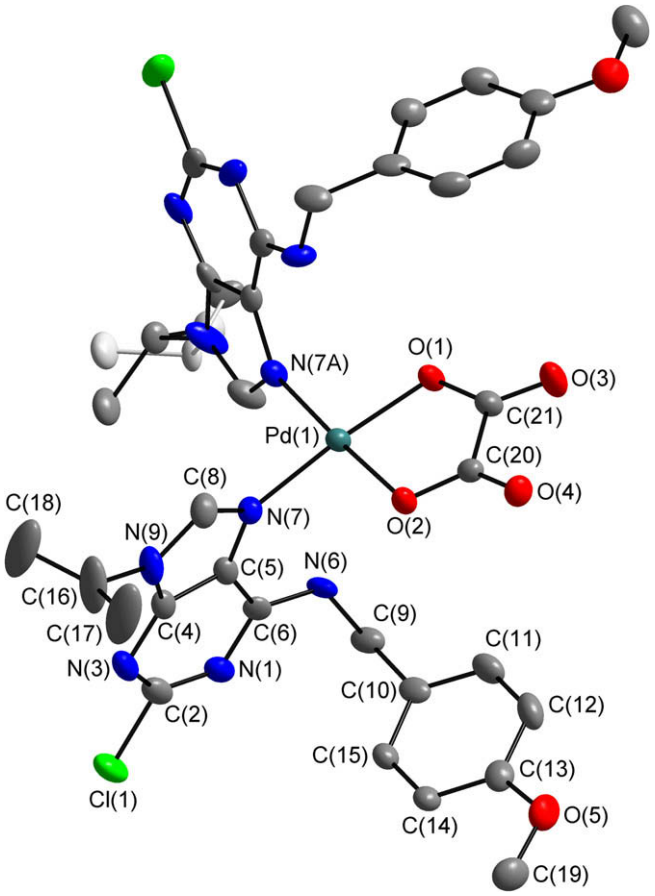

Fig. 1. The molecular structure of $[Pd(L^2)_2(ox)]$ (**2**) with non-hydrogen atoms drawn as thermal ellipsoids at 50% probability level, showing the atom numbering scheme. The C-atoms of isopropyl group distorted over two positions are displayed in light grey colour. H-toms are omitted for clarity.

N(7A) atom]. Moreover, the purine moieties form the dihedral angles of 85.90(7)° ($L^5_{N(7)}$) and 66.18(6)° ($L^5_{N(7A)}$) with a least-square plane formed by atoms of the PdN_2O_2 chromophore.

The oxalate dianion is coordinated through two O-atoms, O(1) and O(2), which are −0.006(2) Å for O(1) and −0.038(3) Å for O(2) out of the least-square PdO_2C_2 plane formed by the Pd(1), O(1), O(2), C(20) and C(21) atoms. A quite different situation was observed for the non-coordinated O-atoms of the oxalato group, since O(3) is −0.122(3) Å and O(4) 0.246(3) Å out of the above-mentioned plane. This is most likely caused by the intermolecular N–H···O hydrogen bonds in which the O(4) atoms are involved, as discussed below.

Two molecules of the complex **2** form centrosymmetric dimers which are linked together by the N(6A)–H···O(4) hydrogen bonds (Fig. 2). Both basal planes, formed by the atoms of PdN_2O_2 moieties, are coplanar with the dihedral angle being 0.000(85)°. None of the O(3) atoms in the crystal structure of **2** is involved in the hydrogen bond system. Except for the N–H···O hydrogen bonds, the non-bonding intermolecular interactions of the C–H···O and C···Cl type have been found to stabilize the crystal structure of **2** (for detailed information see Appendix A in Supplementary material).

The asymmetric unit of **5**·L^5·Me_2CO consists of one molecule of the complex $[Pd(L^5)_2(ox)]$, and L^5 and Me_2CO molecules of crystallization. The central Pd(II) ion is four-coordinated (PdN_2O_2 chromophore) in a slightly distorted square-planar geometry with both L^5 molecules mutually arranged in head-to-tail orientation (Fig. 3). However, several relevant differences were observed between the two discussed complexes, which are most probably caused by the different mutual orientation of both L_n ligands within the complexes **2** (head-to-head) and **5** (head-to-tail).

The Pd(1) atom was found to be more deviated [0.0717(3) Å] from the least-square plane formed by the N(7), N(7A), O(1) and O(2) atoms than in case of complex **2**. The L^5 ligands are coordinated through the N(7) atoms of the purine moieties. The significant increase of the C(5)–N(7)–C(8) angle in the coordinated $L^5_{N(7)}$ and ($L^5_{N(7A)}$) molecules [105.0(3)°, and 105.3(3)°, respectively] as compared to that found in the uncoordinated L^5 molecule of crystallization [103.1(3)°]. Moreover, the values of C(5)–N(7)–C(8) angles determined for **2** [105.2(3)° for $L^2_{N(7)}$ and 105.4(3)° for $L^2_{N(7A)}$] correlated very well with those of **5** (Table 4).

Both purine rings form a dihedral angle of 89.03(6)°. The dihedral angle between the purine moiety and benzene ring within each of the coordinated L_5 molecules is 87.72(10)° for $L^5_{N(7)}$, and 84.25(8)° for ($L^5_{N(7A)}$), respectively, which is significantly higher compared to those of **2**. However, the most significant difference between the complexes **2** and **5** was determined for the dihedral angles, 52.85(7)° ($L^5_{N(7)}$) and 58.63(6)° ($L^5_{N(7A)}$), formed by the purine moieties with a least-square plane formed by the atoms of the PdN_2O_2 chromophore, which is caused by the different mutual orientation of L^2 (head-to-head) and L^5 (head-to-tail) molecules in the complexes **2** and **5**.

The O(3) atom is situated 0.027(3) Å and O(4) atom −0.048(2) Å out of the least-square PdO_2C_2 plane. As in the case of **2**, it is due to the N–H···O hydrogen bonds system, in which only the O(4) of the oxalate group is involved.

Similarly to the complex **2**, two molecules of the complex **5** form centrosymmetric dimers with both PdN_2O_2 basal planes nearly coplanar with the dihedral angle being 0.000(75)° (Fig. 4). However, due to the different mutual orientation of two coordinated L^n molecules within the complex **5**, as compared to **2**, the N(6)–H···O(4) and N(6A)–H···O(4) hydrogen bonds are present within the crystal structure of **5** (Table 5). None of the O(3) atoms in the crystal structure of **5**·L^5·Me_2CO is involved in the hydrogen bond system. Except for the N–H···O hydrogen bonds, the non-bonding intermolecular interactions of the C–H···Cl, C–H···N and C–H···O type have been found to stabilize the crystal structure of **5** (for detailed information see Appendix A in Supplementary material). Similarly to two complex molecules, two L^5 molecules of crystallization also form centrosymmetric dimers which are bonded together by a pair of the hydrogen bonds N(6B)–H···N(7B).

The only monomeric palladium(II) oxalato complexes with unidentate N-donor heterocyclic imine, which are deposited in the CSD, are $[Pd(mi)_2(ox)]\cdot H_2O$ [16] and $[Pd(py)_2(ox)]$ [18]. The Pd–O and Pd–N bond lengths and O–Pd–N angles were determined to be 1.997(3) Å, 1.995(3) Å and 174.85(14)° for $[Pd(mi)_2(ox)]\cdot H_2O$ and 2.010(2) Å, 2.015(2) Å and 175.06(9)° for $[Pd(py)_2(ox)]$. These parameters do not differ significantly from those determined for the complexes **2** and **5**·L^5·Me_2CO, which are given in Table 4. As of complexes **2** and **5**·L^5·Me_2CO, the differences in their Pd–O and Pd–N bond lengths can be considered to be non-significant (0.003–0.021 Å). Moreover, O(1)–Pd(1)–O(2) angle is quite comparable for these two palladium(II) complexes, but all the other angles around the central Pd(II) ion, which involve N7 atom, differ by 1.70–5.35°. This is most likely caused by the opposite arrangement of L^n molecules within these complexes, as mentioned above.

3.5. TG/DTA thermal studies

The complexes $[Pd(L^n)_2(ox)]\cdot xH_2O$ (**1**–**5**) were studied by a simultaneous TG/DTA analysis and the results are summarized in Table 6.

TG curves clearly proved that the complexes **1**–**3** and **5** are non-solvated, because the named compounds have been found to be

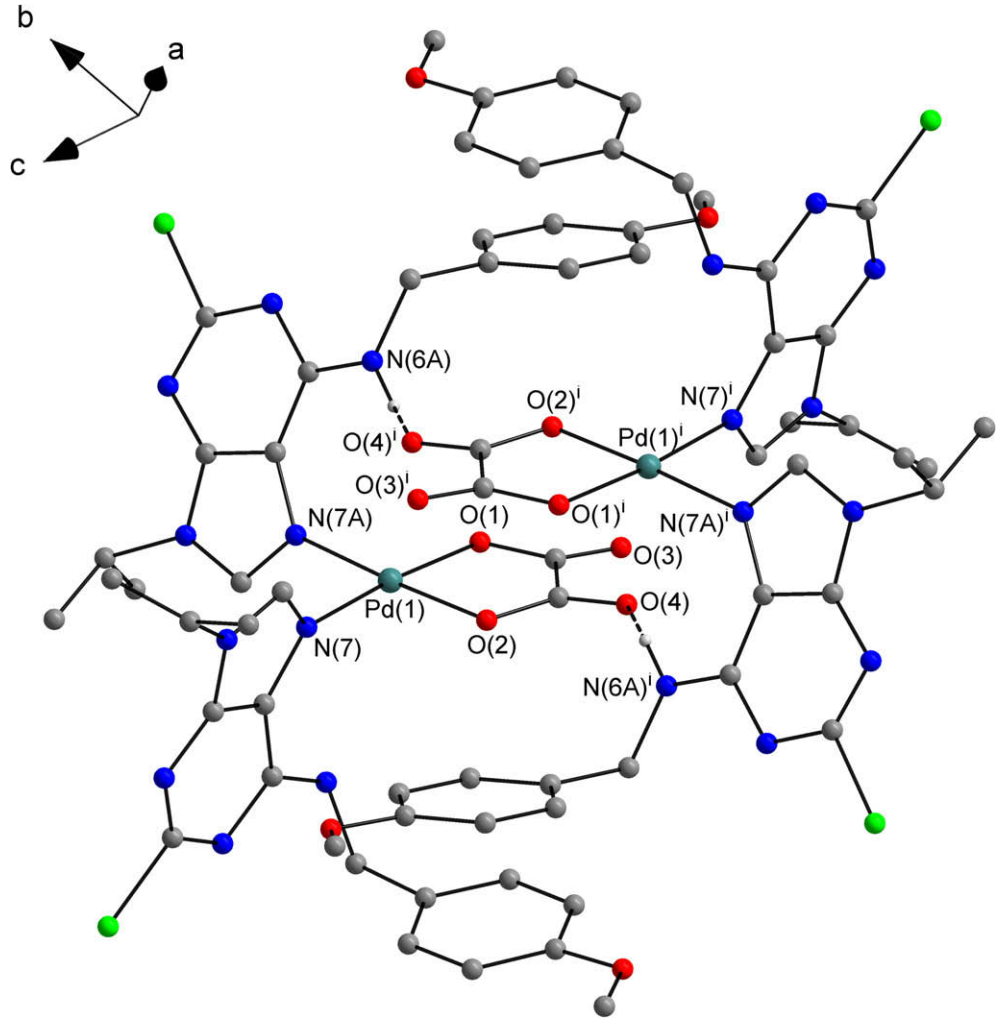

Fig. 2. Part of the crystal structure of $[Pd(L^2)_2(ox)]$ (**2**), showing the N–H···O hydrogen bonds (dashed lines). H-toms not involved into hydrogen bonding are omitted for clarity. Symmetry code: (i) $1-x$, $1-y$, $1-z$.

thermally stable up to 166–177 °C (Fig. 5). Complex **4** has been determined as a dihydrate. The thermal decomposition of this complex started at 66 °C by the loss of the first of the two water molecules of crystallization. The process continued by the elimination of the second water molecule and finished at 145 °C. The loss of both water molecules was accompanied by a weight loss on TG curve (Calc./Found: 3.8/4.0%) and by two *endo*-effects with minima at 100 °C and 134 °C on the DTA curve. The courses of thermal degradations of non-solvated complexes **1**–**5** were nearly identical. The decomposition processes started at 145–177 °C and proceeded without formation of any thermally stable products up to ca. 440 °C, and they were accompanied by two subsequent *exo*-effects on the DTA curves. The differences between the overall weight losses determined by the thermal analyses and those calculated to PdO as the final product of thermal degradation did not differ by more than 1.1% (Table 6).

It should be noted that one more weight loss was observed on the TG curve in case of **1**, **4** and **5**, for which the TG/DTA study was performed up to 1000 °C. The process started at about 810 °C and it was accompanied by a weak *endo*-effect on the DTA curve. This may be attributed to the decomposition of PdO to Pd, as proved by the values of weight loss (Calc./Found: **1**, 2.0/1.8; **4**, 1.7/1.6; **5**, 1.9/1.8%). Thus, PdO and Pd can be considered to be the final products of thermal degradation of $[Pd(L^n)_2(ox)]\cdot xH_2O$ complexes **1**–**5** depending on the temperature range of the experiment.

3.6. In vitro cytotoxicity

All of the prepared palladium(II) oxalato complexes **1**–**5** have been tested on their *in vitro* cytotoxicity against human chronic myelogenous leukaemia (K562) and human breast adenocarcinoma (MCF7) cancer cell lines. The results are expressed as the IC_{50} values and are summarized in Table 7. The tests were performed with the solutions of the complex concentrations up to 25 μM. Significant *in vitro* cytotoxicity has been found for the complexes **3** and **5** on the MCF7 cancer cell line. The determined IC_{50} values of these complexes, 6.2 μM for **3** and 6.8 μM for **5**, are considerably lower than those of the commercially used antineoplastic drugs cisplatin (IC_{50} = 11 μM) and oxaliplatin (IC_{50} = 18 μM) on the same cell line. As for the K562 cancer cell line, the lowest IC_{50} value (16.2 μM) was determined for complex **5**. All the remaining results showed the prepared palladium(II) complexes to be inactive against the mentioned cell line within the evaluated concentration interval, i.e. up to 25 μM.

Nevertheless, the discussed IC_{50} values regarding *in vitro* cytotoxicity of complex **3** against the MCF7 cell line and those of complex **5** against both MCF7 and K562 cell lines are significantly lower than those of *cis*- or *trans*-$[Pd(L)_2Cl_2]$ complexes involving the 2-chloro-N6-(benzyl)-9-isopropyladenine skeleton which were previously prepared in our laboratory [11,42]. Based on these results it is possible to support the positive role of an oxalate anion

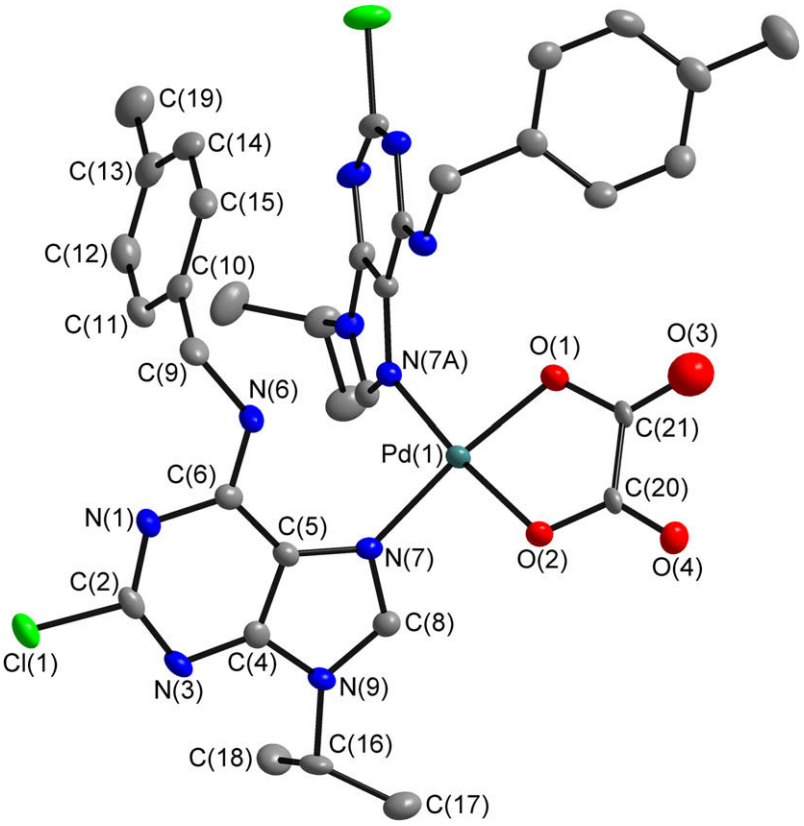

Fig. 3. The molecular structure of $[Pd(L^5)_2(ox)]\cdot L^5\cdot Me_2CO$ (**5**·L^5·Me_2CO) with non-hydrogen atoms drawn as thermal ellipsoids at 50% probability level, showing the atom numbering scheme. The L^5 and Me_2CO molecules of crystallization and H-atoms are omitted for clarity.

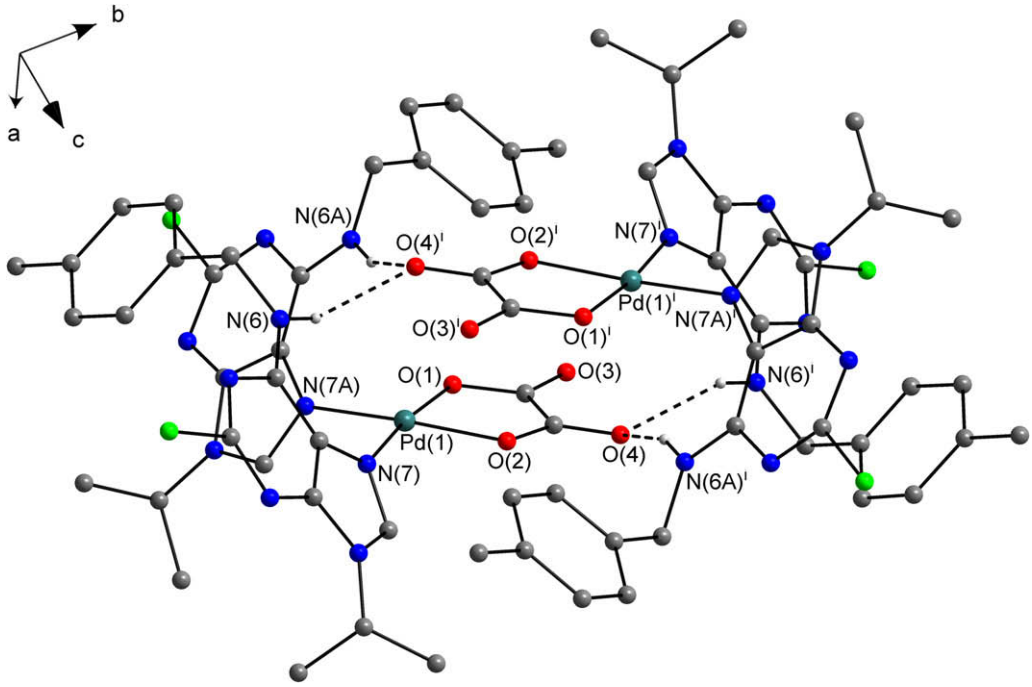

Fig. 4. Part of the crystal structure of $[Pd(L^5)_2(ox)]\cdot L^5\cdot Me_2CO$ (**5**·L^5·Me_2CO), showing the N–H···O hydrogen bonds (dashed lines). The L^5 and Me_2CO molecules of crystallization and H-atoms not involved in hydrogen bonds are omitted for clarity. Symmetry code: (i) $1-x, 1-y, 1-z$.

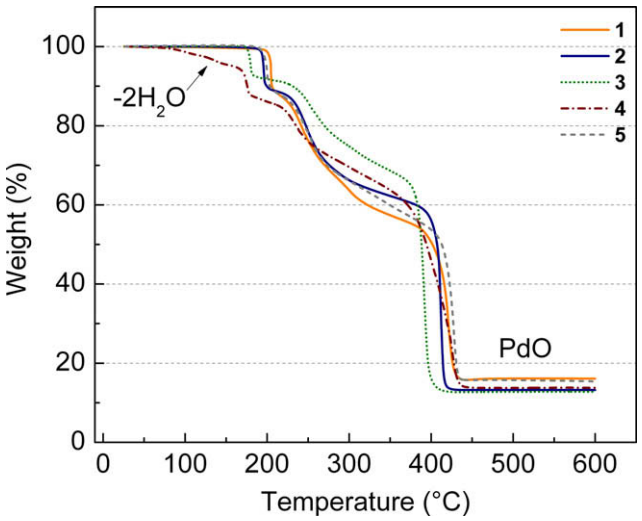

Fig. 5. TG curves of the palladium(II) complexes **1**–**5**.

Table 7
Results of *in vitro* cytotoxicity testing of complexes **1**–**5**.

Complex	IC_{50} (μM)	
	K562[a]	MCF7[b]
$[Pd(L^1)_2(ox)]$ (**1**)	>25	>25
$[Pd(L^2)_2(ox)]$ (**2**)	>12.5	>12.5
$[Pd(L^3)_2(ox)]$ (**3**)	>25	6.2
$[Pd(L^4)_2(ox)]\cdot 2H_2O$ (**4**)	>12.5	>12.5
$[Pd(L^5)_2(ox)]$ (**5**)	16.2	6.8
cisplatin	4.7	10.9
oxaliplatin	8.8	18.2

[a] Human chronic myelogenous leukaemia.
[b] Human breast adenocarcinoma.

as a leaving group on cytotoxic properties of the palladium(II) complexes.

4. Conclusions

The first square-planar palladium(II) oxalato complexes of the composition $[Pd(L^n)_2(ox)]\cdot xH_2O$ ($x = 0$ or 2) (**1**–**5**), bearing adenine-based ligands involving the N6-(benzyl)adenine moiety (L^n), have been prepared by the reactions of $[K_2Pd(ox)_2]\cdot 2H_2O$ with the corresponding L^n compound. Two L^n ligands are coordinated to Pd(II) ion through the N7 atoms of the purine moiety, while the oxalate dianion is coordinated as a bidentate O-donor ligand, as proved by a single crystal X-ray analysis and multinuclear NMR study. The mutual arrangement of two L^n ligands was determined by a single crystal X-ray analysis as head-to-head and head-to-tail orientation in the case of complexes **2**, and **5**, respectively. The *in vitro* cytotoxicity results, expressed as IC_{50} values, obtained for the complexes **3** ($IC_{50} = 6.2$ μM) and **5** ($IC_{50} = 6.8$ μM) on the MCF7 human cancer cell line are significantly lower than those of cisplatin ($IC_{50} = 11$ μM) and oxaliplatin ($IC_{50} = 18$ μM) for the same cancer cell line.

Acknowledgements

The authors gratefully thank the Ministry of Education, Youth and Sports of the Czech Republic for financial support (a Grant No. MSM6198959218), Dr. Miroslava Matíková-Malarová for FTIR and Raman spectra measurements, Mr. Lukáš Dvořák for performing CHN elemental analyses, and Dr. Vladimír Kryštof and Mrs. Dita Parobková for *in vitro* cytotoxicity testing.

Appendix A. Supplementary material

Additional crystallographic data are deposited as CCDC 716051 {$[Pd(L^2)_2(ox)]$ (**2**)} and CCDC 716052 {$[Pd(L^5)_2(ox)]\cdot L^5\cdot Me_2CO$ (**5**$\cdot L^5\cdot Me_2CO$)} and can be obtained free of charge from the Cambridge Crystallographic Data Centre, 12 Union Road, Cambridge CB2 1EZ, UK; fax: (+44) 1223 336 033; email: deposit@ccdc.cam.ac.uk, or at http://www.ccdc.cam.ac.uk. The results of elemental analyses and FTIR, Raman and NMR (^1H, ^{13}C, ^{15}N) spectral data of L^1–L^5 organic compounds, the results of FTIR, Raman and NMR (^1H, ^{13}C, ^{15}N) spectroscopies of the complexes **1**–**5**, as well as the figures of crystal packing of the complexes **2** and **5**$\cdot L^5\cdot Me_2CO$ together with the tables of its selected parameters are deposited. Supplementary material associated with this article can be found, in the online version, at doi:10.1016/j.jinorgbio.2009.04.008.

References

[1] B. Rosenberg, L. Van Camp, T. Krigas, Nature 205 (1965) 698–699.
[2] L.R. Kelland, N.P. Farrell, Platinum-Based Drugs in Cancer Therapy, Humana, Totowa, 2000.
[3] K.R. Harrap, Cancer Treat. Rev. 12 (1985) 21–33.
[4] Y. Kidani, K. Inagaki, J. Med. Chem. 21 (1978) 1315–1318.
[5] L.M. Pasetto, R.M. DAndrea, A.A. Brandes, E. Rossi, S. Monfardini, Crit. Rev. Oncol. Hematom. 60 (2006) 59–75.
[6] J.L. Butour, S. Wimmer, F. Wimmer, P. Castan, Chem. Biol. Interact. 104 (1997) 165–178.
[7] M. Gielen, E.R.T. Tiekink, Metallotherapeutic Drugs and Metal-Based Diagnostic Agents, Willey, London, 2005. pp. 399–419.
[8] A. Garoufis, S.K. Hadjikakou, N. Hadjiliadis, Coord. Chem. Rev. (2008), doi:10.1016/j.ccr.2008.09.011.
[9] J. Kuduk-Jaworska, A. Puszko, M. Kubiak, M. Pełczyńska, J. Inorg. Biochem. 98 (2004) 1447–1456.
[10] S. Ray, R. Mohan, J.K. Singh, M.K. Samantaray, M.M. Shaikh, D. Panda, P. Ghosh, J. Am. Chem. Soc. 129 (2007) 15042–15053.
[11] L. Szüčová, Z. Trávníček, M. Zatloukal, I. Popa, Bioorg. Med. Chem. 14 (2006) 479–491.
[12] M.J. Cleare, Coord. Chem. Rev. 12 (1974) 349–405.
[13] E. Monti, M. Gariboldi, A. Maiocchi, E. Marengo, C. Cassino, E. Gabano, D. Osella, J. Med. Chem. 48 (2005) 857–866.
[14] F.G. Mann, D. Crowfoot, D.C. Gattiker, N. Wooster, J. Chem. Soc. (1935) 1642–1652.
[15] G. Devoto, M. Biddau, M. Massacesi, R. Pinna, G. Ponticelli, L.V. Tatjanenko, I.A. Zakharova, J. Inorg. Biochem. 19 (1983) 311–318.
[16] Z. Zhou, G. Hu, K. Yu, L. Liu, W.T. Robinson, L. Zhang, Q. Yang, G. Li, Chinese J. Struct. Chem. 6 (1987) 119–121.
[17] K.I. Lee, T. Tashiro, M. Noji, Chem. Pharm. Bull. 42 (1994) 702–703.
[18] S. Dey, P. Banerjee, S. Gangopadhyay, P. Vojtíšek, Transit. Met. Chem. 28 (2003) 765–771.
[19] A.S. Abu-Surrah, T.A.K. Al-Allaf, M. Klinga, M. Ahlgren, Polyhedron 22 (2003) 1529–1534.
[20] M. Odoko, Y. Wang, N. Okabe, Acta Crystallogr. Sect. E 60 (2004) m1825–m1827.
[21] M. Odoko, N. Okabe, Acta Crystallogr. Sect. E 63 (2007) m628–m630.
[22] F.A. Allen, Acta Crystallogr. Sect. B: Struct. Sci. 58 (2002) 380–388.
[23] M. Quirós, J.M. Salas, M. Purificación Sánchez, A.L. Beauchamp, X. Solans, Inorg. Chim. Acta 203 (1994) 213–220.
[24] A. Garoufis, K. Karidi, N. Hadjiliadis, S. Kasselouri, J. Kobe, J. Balzarini, E. De Clercq, Met. Based Drugs 8 (2001) 57–63.
[25] W.M. Beck, J.C. Calabrese, N.D. Kottmair, Inorg. Chem. 18 (1979) 176–182.
[26] K.J. Barnham, C.J. Bauer, M.I. Djuran, M.A. Mazid, T. Rau, P.J. Sadler, Inorg. Chem. 34 (1995) 2826–2832.
[27] P.J. Davies, Plant Hormones, third ed., Springer, Dordrecht, 1997.
[28] L. Meijer, A. Borgne, O. Mulner, J.P. J Chong, J.J. Blow, N. Inagaki, M. Inagaki, J.G. Delcros, J.P. Moulinoux, Eur. J. Biochem. 243 (1997) 527–536.
[29] C. Benson, S. Kaye, P. Workman, M. Garret, M. Walton, J. de Bono, Br. J. Cancer 92 (2005) 7–12.
[30] CrysAlis RED and CrysAlis CCD software (Ver.1.171.23), Oxford Diffraction: Oxford, UK, 2003.
[31] G.M. Sheldrick, SHELXS 97, Acta Cryst. A 46 (1990) 467.
[32] G.M. Sheldrick, SHELXL 97, Program for Crystal Structure Refinement, University of Göttingen, Göttingen, Germany, 1997.
[33] K. Brandenburg, DIAMOND, Relase 3.1f, Crystal Impact GbR, Bonn, Germany, 2006.
[34] K. Torigoe, K. Esumi, Langmuir 9 (1993) 1664–1667.

[35] C.H. Oh, S.C. Lee, K.S. Lee, E.R. Woo, C.Y. Hong, B.S. Yang, D.J. Baek, J.H. Cho, Arch. Pharm. Pharm. Med. Chem. 332 (1999) 187–190.
[36] W.J. Geary, Coord. Chem. Rev. 7 (1971) 81–122.
[37] C.J. Pouchert, in: The Aldrich Library of Infrared Spectra, Aldrich Chemical Company Press, Milwaukee, 1981.
[38] D.M. de Faria, M.I. Yoshida, C.B. Pinheiro, K.J. Guedes, K. Krambrock, R. Diniz, L.F.C. de Oliveira, F.C. Machalo, Polyhedron 26 (2007) 4525–4532.
[39] J. Fujita, A.E. Martell, K. Nakamoto, J. Chem. Phys. 36 (1962) 324–331.
[40] K. Nakamoto, Infrared and Raman Spectra of Inorganic and Coordination Compounds, Part B: Applications in Coordination, Organometallic and Bioinorganic Chemistry, fifth ed., Willey, New York, 1997.
[41] Z. Dhaouadi, M. Ghomi, J.C. Austin, R.B. Girling, R.E. Hester, P. Mojzes, L. Chinsky, P.Y. Turpin, C. Coulombeau, H. Jobic, J. Tomkinson, J. Phys. Chem. 97 (1993) 1074–1084.
[42] Z. Trávníček, L. Szüčová, I. Popa, J. Inorg. Biochem. 101 (2007) 477–492.